Available online at www.sciencedirect.com
SCIENCE DIRECT®
Thin Solid Films 496 (2006) 234 – 239
thin solid films
www.elsevier.com/locate/tsf

Low temperature photoluminescence and infrared dielectric functions of pulsed laser deposited ZnO thin films on silicon

S. Heitsch [a], C. Bundesmann [a], G. Wagner [b], G. Zimmermann [a], A. Rahm [a], H. Hochmuth [a], G. Benndorf [a], H. Schmidt [a], M. Schubert [a], M. Lorenz [a,*], M. Grundmann [a]

[a] Universität Leipzig, Fakultät für Physik und Geowissenschaften, Institut für Experimentelle Physik II, Linnéstr. 5, 04103 Leipzig, Germany
[b] Institut für Nichtklassische Chemie e.V. an der Universität Leipzig, Permoserstr. 15, 04318 Leipzig, Germany

Received 12 January 2005; received in revised form 28 July 2005; accepted 18 August 2005
Available online 16 September 2005

Abstract

C-axis oriented ZnO thin films were grown on silicon (100) and (111) substrates by pulsed laser deposition. Low temperature photoluminescence spectra show besides the peaks of free excitons, of defect bound excitons, and of a donor–acceptor pair transition a new doublet at 3.328/3.332 eV. The doublet seems to originate from the columnar textured ZnO film structure. A corresponding structural dependence of the broadening parameter of the infrared dielectric functions was derived from spectroscopic ellipsometry in the spectral range from 380 to 1200 cm^{-1}. The wave numbers of the E_1 transverse optical and A_1 longitudinal optical phonon modes of the ZnO films on silicon are determined to be 406 and 573 cm^{-1}, respectively. These values are slightly smaller than those of single-crystalline ZnO thin films on sapphire.

PACS: 78.30.Fs; 78.55.Et; 81.05.Dz; 81.15.Fg
Keywords: Zinc oxide; Thin films; Luminescence; Infrared ellipsometry; Pulsed laser deposition

1. Introduction

Currently, the wide-band gap II–VI semiconductor zinc oxide is gaining much interest due to its promising optical, electrical, and magnetic properties and the state of the art techniques to grow high quality ZnO single crystals and thin films [1]. The use of silicon substrates allows the integration of II–VI optoelectronic devices with silicon-based electronics. Therefore, the growth and characterization of ZnO thin film structures on silicon substrates were extensively studied [2–12]. Recently, a variety of methods turned out to be suitable procedures for the direct growth of *c*-axis oriented ZnO thin films on Si substrates, such as chemical vapor deposition [2,3], cathodic arc deposition [4], molecular beam epitaxy [5], and magnetron sputtering [6–8]. Also pulsed laser deposition (PLD) has proven to be an adequate preparation method for ZnO thin films on Si [9–12]. PLD is an extremely flexible deposition technique and allows easy doping and alloying of ZnO thin films [13]. Furthermore, PLD grown ZnO films on sapphire substrates showed very high electron mobilities up to 155 cm^2/Vs at 300 K and photoluminescence (PL) excitonic peak widths as small as 1.2 meV at 2 K [14]. Thus, in general, a high quality of PLD grown ZnO thin films is confirmed.

The luminescence spectra of ZnO thin films on silicon have been recorded at room temperature [2–4,6–8,12,13] and at temperatures down to 77 K [2]. In addition, very few PL experiments have been performed down to temperatures of 6 to 13 K [5–7,10]. However, some of the low temperature PL spectra do not show much details of the PL emission. Therefore, in the following detailed PL spectra recorded at 2 K of PLD ZnO thin films on silicon substrates are presented, which correlate to the growth condition dependent structure of the films. Second, to the best of our knowledge, the first investigations of the infrared dielectric functions of ZnO thin films on silicon by spectroscopic ellipsometry [15] are presented here. X-ray diffraction (XRD), atomic force microscopy (AFM), and high-resolution transmission electron microscopy (HRTEM) were used to illustrate the crystalline structure of the thin films.

* Corresponding author.
E-mail address: mlorenz@physik.uni-leipzig.de (M. Lorenz).

0040-6090/$ - see front matter © 2005 Elsevier B.V. All rights reserved.
doi:10.1016/j.tsf.2005.08.305

2. Experimental details

ZnO thin films were prepared by PLD [13,14] on Si (111) and Si (100) substrates. Although the natural SiO_x film on the substrates was removed prior to their insertion in the PLD chamber by standard HF etching, the following deposition under oxidizing conditions seems to promote the coverage of the substrate with a thin SiO_x film, as shown below in Figs. 2 and 3 in the HRTEM cross sections. The substrate temperature was controlled by the applied heater power. This was varied from 300 to 600 W corresponding approximately to a substrate temperature range from 500 to 675 °C. The oxygen partial pressure during PLD growth was varied from 3×10^{-2} to 10 Pa. For more details about our PLD process including target preparation see Refs. [13,14]. XRD $2\Theta-\omega$ scans and rocking curves were measured using the $Cu-K_{\alpha 1}$ line in a Philips X'Pert in parallel beam geometry without analyzer crystal. AFM in tapping mode was performed using a Nanoscope IV/Dimension 3100 from Veeco Metrology. The scan speed was 5 μm/s with a sampling rate of 256 samples/s. Si tips were used for the measurements with an engagement ratio of 0.8. TEM and HRTEM were done with a Philips CM-200 at an accelerating voltage of 200 kV. The samples were prepared for $(111)_{Si}$ respectively $(100)_{Si}$ plane view observations as well as for $(110)_{Si}$ cross section observations by mechanical grinding, dimpling, and finally by Ar^+ ion milling at an accelerating voltage of 4 kV and a beam current of 0.5 mA. The beam incidence angle was 13°.

Infrared spectroscopic ellipsometry (IRSE) experiments [15] were performed with a variable-polarizer, rotating-compensator type spectroscopic ellipsometer under an angle of incidence of $\Phi_a=50°$ and 70° [15,16]. Spectroscopic ellipsometry is a well-known technique for the determination of the dielectric function and thickness d of thin films within layered samples. The ellipsometric parameters Ψ and Δ are related to the complex reflectance ratio ρ by $\rho\equiv r_p/r_s=\tan\Psi\exp i\Delta$, where r_p and r_s are the reflection coefficients for light polarized parallel (p), and perpendicular (s) to the plane of incidence, respectively. IRSE spectra are analyzed by model calculations, where the layered structure of the samples is considered appropriately [15]. The infrared dielectric function is sensitive to phonon and free-charge-carrier contributions. No free-charge-carrier contribution was detected in any of the ZnO thin films on silicon, and hence a simple harmonic oscillator model with Lorentzian broadening was used for the model dielectric functions

$$\varepsilon_j(\omega)=\varepsilon_{\infty,j}\frac{\omega_{LO,j}^2-\omega^2-i\omega\gamma_j}{\omega_{TO,j}^2-\omega^2-i\omega\gamma_j}, \quad (1)$$

where $\omega_{TO,j}$ and $\omega_{LO,j}$ are the frequencies of the transverse optical (TO) and longitudinal optical (LO) phonon modes, respectively, and γ_j is the corresponding lattice mode broadening parameter. The parameter $\epsilon_{\infty,j}$ denotes the high-frequency model dielectric function limit. Because the ZnO thin films possess a hexagonal crystal structure, dielectric functions for light polarized perpendicular (subscript $j=\perp$) and parallel ($j=\parallel$) to the optical c-axis have to be distinguished. The phonons with E_1- and A_1-symmetry of a crystal with wurtzite structure are represented by the subscript $j=\perp$ and $j=\parallel$, respectively. PL measurements were done at 2 K with the 325 nm line of a continuous wave HeCd laser as excitation source. The laser spot size was about 100 μm and the corresponding laser power at the samples was approximately 7 mW. The photoluminescence radiation was spectrally resolved by a 320 mm monochromator and detected by a photomultiplier.

3. Results and discussion

XRD $2\Theta-\omega$ scans of typical ZnO thin films grown on Si (111) and Si (100) substrates show within the given range of growth parameters only the ZnO (0002) and (0004) diffraction peaks which means that all films are wurtzite type and c-axis oriented. The ZnO (0002) reflection has a full width at half maximum (FWHM) of 0.17° ($2\Theta-\omega$) and the width of the corresponding rocking curve (ω-scan) is 0.87°. These values are among the best values reported for ZnO films on silicon so far [2,11,13]. For comparison, reference ZnO films on c-plane sapphire had a FWHM of 0.12° and 0.1°, respectively. In contrast to ZnO films grown on sapphire [13,14], XRD ϕ-scans revealed no in-plane orientation of the ZnO films on silicon. Examples for the results of AFM measurements are shown in Fig. 1. In all images ZnO columns with different heights are obvious. Fig. 1(a–c) shows images of three samples grown on Si (100) under an oxygen pressure of 1 Pa with substrate temperatures of 500, 620, and 675 °C, respectively. The average roughness at 10×10 μm^2 film area was 18, 36, and 48 nm, respectively. Obviously, the diameter of the columns and the roughness increases with rising growth temperature. Similar behavior was found for our samples grown on Si (111) substrates, however, the average roughness was in the range from 6 to 17 nm only. A dependence of the grain diameter on the oxygen pressure applied during growth could not be observed.

Figs. 2 and 3 show TEM and HRTEM images, partly together with the corresponding selected area diffraction (SAD) images, of PLD ZnO films grown on Si (111) and Si (100) substrates, respectively. Figs. 2(a) and 3(a) show bright field $(111)_{Si}$ and $(100)_{Si}$ plane view observations, the average grain size is about 70 and 100 nm, respectively. Note that the SAD image of the film on Si (111) was taken from many columns as indicated in Fig. 2(a), in contrast to the SAD image in Fig. 3(a) which was taken from a few single grains only. Therefore, the ZnO columns on both Si (111) and Si (100) show no preferential azimuthal in-plane orientation relating to the (111) or (100) oriented Si substrate. Fig. 2(b) shows a HRTEM lattice image with intermediate amorphous SiO_x layer of 2 to 4 nm thickness and an additional interdiffusion zone of silicon suboxides with the first ZnO monolayers as proposed in Ref. [17]. Fig. 3(b) depicts a $(100)_{Si}$ plane-view HRTEM image of grain boundaries between three ZnO columns. Figs. 2(c) and 3(c) are both bright field $(110)_{Si}$ TEM cross sections of ZnO on Si (111)

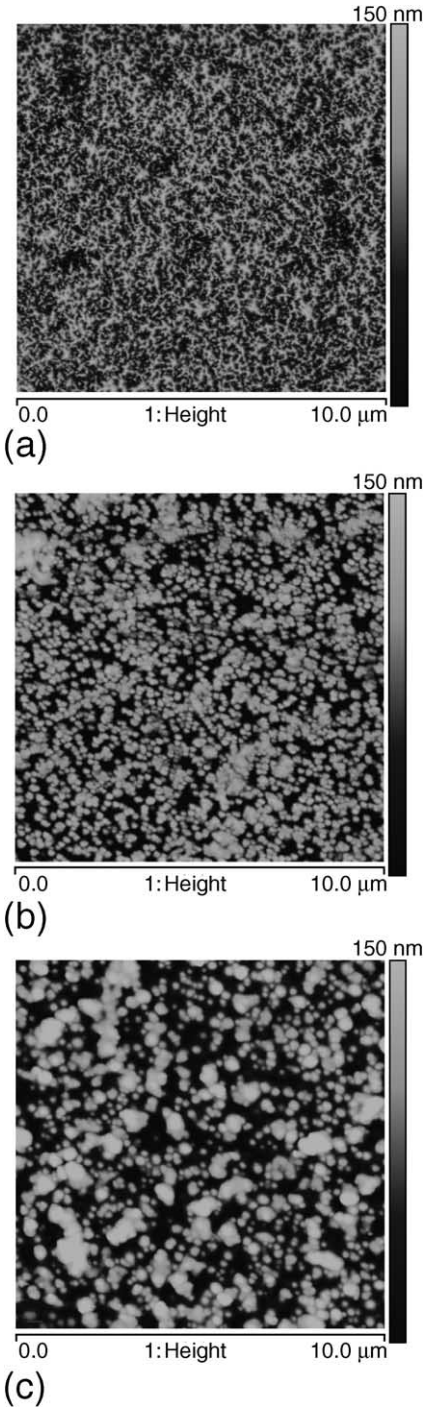

Fig. 1. AFM scan images of three ZnO thin films grown on Si (100) with a heater power (substrate temperature) of (a) 300 W (~500 °C), (b) 500 W (~620 °C), and (c) 600 W (~675 °C), respectively.

and Si (100), respectively. The insets show the SAD patterns taken from one single ZnO column and the underlying part of the Si substrate simultaneously. The intermediate SiO_x interface layer is clearly visible again. The existence of this layer between the substrate and the actual thin film is most probably the reason for the very similar crystalline structure of our ZnO thin films grown on Si (111) and on Si (100) substrates. These findings correspond to the detailed HRTEM and SAD investigations [9], where a similar *c*-axis oriented

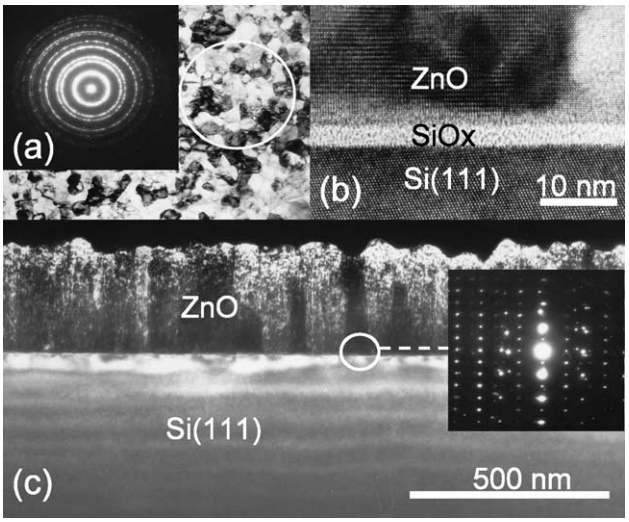

Fig. 2. TEM images and SAD patterns (insets) of a polycrystalline ZnO film on silicon (111) grown at 10^{-1} Pa: (a) bright field $(111)_{Si}$ plane view observation, grain size is about 70 nm, (b) cross section HRTEM lattice image with intermediate SiO_x layer, and (c) weak beam $(110)_{Si}$ TEM cross section. The areas from which the SAD patterns were taken are within the white circles.

ZnO growth was reported on Si (100), Si (111), glass, and SiO_2/Si (100) substrates. In Figs. 2(c) and 3(c), the columnar structure of the ZnO thin films is clearly visible. The different brightness of the various columns is caused by their dissimilar in-plane orientation. Within the columns the images show lines running in growth direction. These are representing dislocations in the grains indicating that the crystalline quality of the resulting thin films is limited.

The IRSE data are analyzed with a three-phase-model (ambient/thin film/substrate) with the dielectric function in Eq. (1) for the ZnO thin film and a constant for the dielectric function of the silicon substrate. As for all *c*-plane hexagonal thin films, the A_1(TO) mode wave number is not accessible by

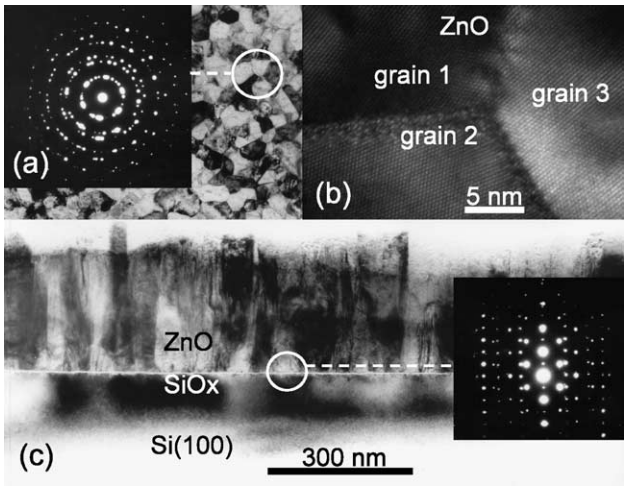

Fig. 3. TEM images and SAD patterns (insets) of a polycrystalline ZnO film on silicon (100) grown at 1 Pa: (a) bright field $(100)_{Si}$ plane view observation, grain size is about 100 nm, (b) $(100)_{Si}$ plane-view HRTEM lattice image of grain boundaries, and (c) bright field $(110)_{Si}$ TEM cross section with intermediate SiO_x interface layer.

IRSE [15]. Because of the relatively low thin film thickness between 300 and 700 nm, IRSE does not provide sensitivity to the wave number of the E_1(LO) mode and the anisotropy of the high-frequency dielectric constant parameters. Therefore, for all ZnO thin films on silicon the A_1(TO) and E_1(LO) mode wave number are set equal to 378 and 590 cm^{-1}, respectively, as for the single-crystalline ZnO thin films on sapphire reported in Ref. [16]. The high-frequency dielectric constant parameters are assumed to be isotropic. Experimental and best-fit model IRSE spectra of the ZnO thin films on silicon (111) substrates grown at different oxygen pressures are plotted in Fig. 4(a)/(b). A good agreement of the experimental and best-fit model spectra can be seen. While the Ψ-spectra look similar for all thin films, the Δ-spectra show a strong variation of the Berreman structure just below 600 cm^{-1}. This variation reflects different phonon mode broadening parameters. In general, a lower crystal quality causes a larger phonon mode broadening parameter. Here it is found that with increasing oxygen pressure the broadening parameter decreases at first until it starts to increase again as soon as a pressure of 3 Pa is exceeded, as shown in Fig. 4(c). Furthermore it is found that with increasing substrate temperature the broadening parameter decreases. Considering that a smaller broadening parameter indicates a better crystal quality, IRSE results suggest that the optimal growth parameters are an oxygen pressure of about 1–3 Pa and a substrate heater power of 600 W. A better crystal quality of the thin films grown at a higher substrate temperature is also found by the AFM investigations in Fig. 1 and the PL spectra in Fig. 6. The best-fit wave numbers of the E_1(TO) and A_1(LO) modes are found to vary only slightly around 406 and 573 cm^{-1}, respectively, for all ZnO thin films on silicon studied here. These values are slightly smaller than those of the single-crystalline thin films (409.1 and 574.5 cm^{-1}, respectively) on sapphire reported in Ref. [16]. The differences are likely related to the polycrystalline structure of the ZnO thin films on silicon.

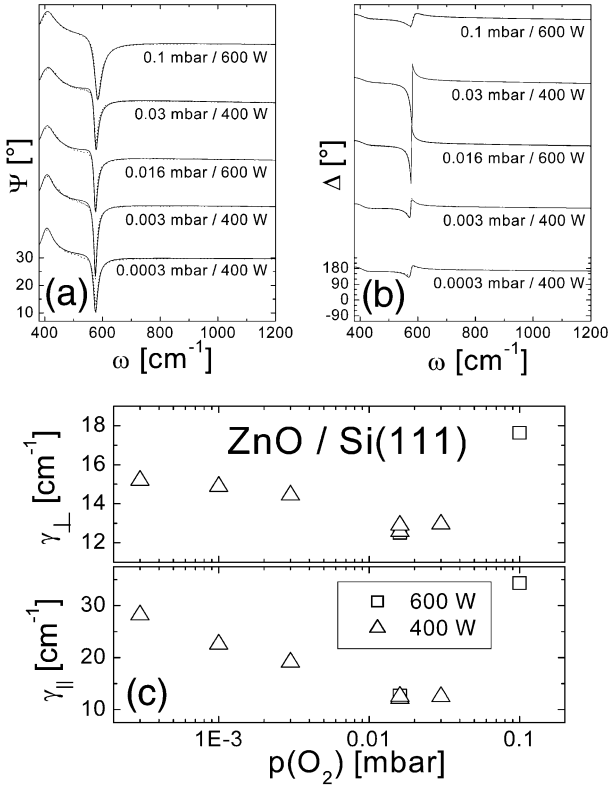

Fig. 4. (a) Ψ- and (b) Δ-spectra, each with experimental (dotted lines) and best-fit model (solid lines) of ZnO thin films on silicon (111) grown with different oxygen pressure and substrate heater power. The corresponding substrate temperature at 400 W is about 580 °C and at 600 W about 675 °C. The angle of incidence in IRSE was 50°. Spectra are shifted for clarity. (c) Best-fit phonon mode broadening parameters γ_j of the IR model dielectric function in Eq. (1) versus oxygen pressure during ZnO thin film growth on silicon (111).

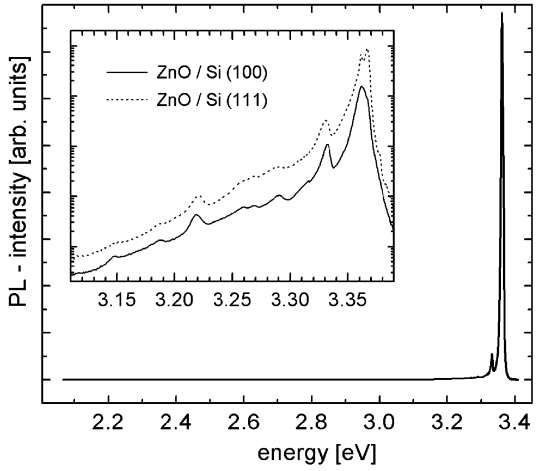

Fig. 5. Low temperature PL spectrum (2 K) of a ZnO thin film grown on Si(100) at $p(O_2)=1$ Pa and 500 W substrate heater power. The inset compares the ZnO/Si(100) near band edge emission with that of ZnO/Si(111) grown at 1.6 Pa and 600 W. The base line is shifted for a better visualization.

PL measurements of the thin films show a strong near band edge emission with negligible emission in the visible spectral range as shown in Fig. 5. Furthermore, the PL spectra of the ZnO thin films grown on Si (100) and Si (111) in the inset of Fig. 5 both contain the same features and resemble each other. This can be understood in terms of the similar crystalline

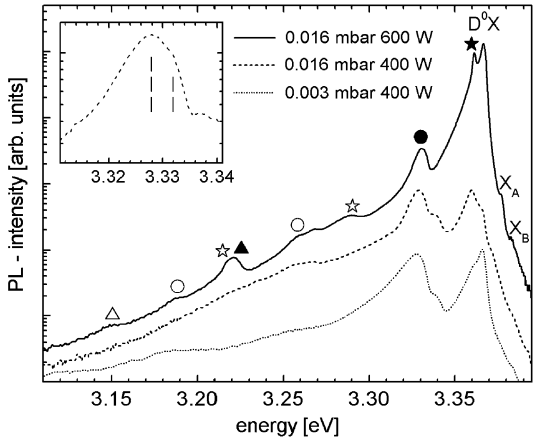

Fig. 6. Near band edge PL spectra (2 K) of three ZnO films grown under different conditions on Si(111) substrates. The baselines are shifted by a factor of 4 with respect to each other. Solid symbols mark zero-phonon transitions, the respective open symbols their phonon replica. The inset shows the doublet around 3.33 eV (marked by the dashed lines) in more detail.

structure of the thin films on the two sorts of substrates (see TEM cross sections in Figs. 2 and 3). Detailed PL near band edge emission spectra of thin films grown under different conditions are depicted in Fig. 6. The sample grown with 600 W heater power and an oxygen pressure of 1.6 Pa shows a spectrum with clearly distinguishable peaks that can be assigned as follows. The emission of free A- and B-excitons, labeled X_A and X_B, is found at energies of 3.377 and 3.384 eV, respectively. The peaks labeled D^0X around 3.36 eV are tentatively assigned to donor bound excitons following Ref. [18]. The corresponding phonon replica are marked by open stars. The peak at 3.33 eV marked by a solid circle is found to be a doublet of two peaks at about 3.328 and 3.332 eV (as shown in the inset of Fig. 6). Meyer et al. [18] assigned the latter one to the emission of excitons bound to structural defects. As the TEM images (Figs. 2 and 3) clearly show structural defects in ZnO thin films grown on silicon, the appearance of this PL peak is not surprising. The zero-phonon transition with lowest energy in the PL spectra of the investigated samples is a peak at about 3.221 eV (solid triangle in Fig. 6). It was previously assigned to a donor–acceptor pair transition [18]. The low temperature PL spectra in Refs. [5,6] show emission peaks peculiar to ZnO films on silicon. However, the PL peaks at 3.317 and 3.28 [5], and 3.09 eV (V_{Zn}) [6] could not be identified in our spectra. Therefore, the explanation of the manifold luminescence emission of ZnO thin films with polycrystalline or textured structure has to take into account the structural details based on the growth history of the samples.

The PL spectra of samples grown under different conditions show remarkable differences. Fig. 6 indicates clearly that the dominating factor concerning the intensity of the emission of the donor bound excitons relative to all other features in the spectrum is the growth temperature. With increasing growth temperature the intensities of the D^0X peaks increase, while in general the features of the PL spectrum become more defined. Optimal heater powers concerning the emission properties were found to be 500 to 600 W, which agree well with the optimum value of 600 W suggested by the IRSE results. These parameters correspond to approximate substrate temperatures of 620–675 °C. Different oxygen pressures during film growth do not lead to such obvious changes in the emission properties. Note that the shape and position of the doublet around 3.33 eV are different for all three samples shown in Fig. 6. In fact, there is a tendency of the apparent maximum to shift slightly to higher energies when the growth parameters approach the optimum values found in the IRSE experiments. In samples grown at low temperature and low oxygen pressure the 3.328 eV peak dominates over the second peak of the doublet. However, its influence on the position and width of the doublet decreases with increasing growth temperature as well as with increasing oxygen pressure during growth. This means that with increasing growth temperature and oxygen pressure the intensity and line width of the PL peak at 3.328 eV slightly decreases. This behavior is consistent with that of the broadening parameter from the IRSE measurements. Therefore, the origin of the peak at 3.328 eV is correlated with the crystal quality of the samples and may be connected to defects like dislocations or grain boundaries.

4. Summary

ZnO thin films were grown on Si (111) and Si (100) substrates by PLD at growth temperatures from 500 to 675 °C and oxygen pressures from 3×10^{-2} to 10 Pa. XRD, AFM, and TEM investigations show that all films have a columnar structure and are *c*-axis oriented. The diameter of the columns becomes larger with increasing growth temperature, while no explicit dependence of the grain size on the oxygen pressure can be found. IRSE measurements suggest that the best crystal quality is obtained when the substrate temperature is approximately 675 °C and the partial oxygen pressure lies between 1 and 3 Pa. In this growth parameter range also optimal PL emission properties can be observed with clearly distinguishable peaks and the dominating emission originating from donor bound excitons. At 3.328/3.332 eV a new PL doublet has been found, the intensities and line widths of the doublet peaks depend on the growth conditions and thus on the crystalline quality of the thin films. In thin films grown at optimum conditions, i.e. films with large grains and best crystal quality, its intensity and line width are smallest.

Acknowledgments

This work was supported by the DFG within Research Group 404, project A9, and by the BMBF Young Scientists Group “Nanospintronics” FKZ 03N8708.

References

[1] D.S. Ginley, C. Bright (Eds.), Transparent Conducting Oxides, Materials Research Society Bulletin, vol. 25, 2000, p. 15.
[2] B.S. Li, Y.C. Liu, Z.S. Chu, D.Z. Shen, Y.M. Lu, J.Y. Zhang, X.W. Fan, J. Appl. Phys. 91 (2002) 501.
[3] B. Guo, Z.R. Qui, K.S. Wong, Appl. Phys. Lett. 82 (2003) 2290.
[4] S.F. Yu, C. Yuen, S.P. Lau, Y.G. Wang, H.W. Lee, B.K. Tay, Appl. Phys. Lett. 83 (2003) 4288.
[5] N. Kawamoto, M. Fujita, T. Tatsumi, Y. Horikoshi, Jpn. J. Appl. Phys. 42 (2003) 7209.
[6] S.-H. Jeong, B.-S. Kim, B.-T. Lee, Appl. Phys. Lett. 82 (2003) 2625.
[7] K.-K. Kim, N. Koguchi, Y.-W. Ok, T.-Y. Seong, S.-J. Park, Appl. Phys. Lett. 84 (2004) 3810.
[8] C.-C. Lin, San-Y. Chen, Syh-Y. Cheng, H.-Y. Lee, Appl. Phys. Lett. 84 (2004) 5040.
[9] J.H. Choi, H. Tabata, T. Kawai, J. Cryst. Growth 226 (2001) 493.
[10] M. Kumar, R.M. Mehra, A. Wakahara, M. Ishida, A. Yoshida, J. Appl. Phys. 93 (2003) 3837.
[11] F.K. Shan, B.C. Shin, S.W. Jang, Y.S. Yu, J. Eur. Ceram. Soc. 24 (2004) 1015.
[12] S.S. Kim, B.T. Lee, Thin Solid Films 446 (2004) 307.
[13] M. Lorenz, E.M. Kaidashev, H. von Wenckstern, V. Riede, C. Bundesmann, D. Spemann, G. Benndorf, H. Hochmuth, A. Rahm, H.-C. Semmelhack, M. Grundmann, Solid-State Electron. 47 (2003) 2205.
[14] E.M. Kaidashev, M. Lorenz, H. Wenckstern, A. Rahm, H.-C. Semmelhack, K.-H. Han, G. Benndorf, C. Bundesmann, H. Hochmuth, M. Grundmann, Appl. Phys. Lett. 82 (2003) 3901.

[15] M. Schubert, Infrared Ellipsometry on Semiconductor Layer Structures: Phonons, Plasmons and Polaritons, Springer, Berlin, 2004.
[16] N. Ashkenov, B.N. Mbenkum, C. Bundesmann, V. Riede, M. Lorenz, D. Spemann, E.M. Kaidashev, A. Kasic, M. Schubert, M. Grundmann, G. Wagner, H. Neumann, V. Darakchieva, H. Arwin, B. Monemar, J. Appl. Phys. 93 (2003) 126.
[17] V. Craciun, J.M. Howard, D. Craciun, R.K. Singh, Appl. Surf. Sci. 208–209 (2003) 507.
[18] B.K. Meyer, H. Alves, D.M. Hofmann, W. Kriegseis, D. Forster, F. Bertram, J. Christen, A. Hoffmann, M. Straβburg, M. Dworzak, U. Haboeck, A.V. Rodina, Phys. Status Solidi, B Basic Res. 241 (2004) 231.